

Image Registration Exploiting Five-point Coplanar Perspective Invariant and Maximum-Curvature Point

P. Putjarupong[†], C. Pintavirooj[†], W. Withayachumnankul[‡], M. Sangworasil[†]

[†]Research Center for Communication and Information Technology (ReCCIT), and
Department of Electronics, Faculty of Engineering,

[‡]Department of Information Engineering, Faculty of Engineering,
King Mongkut's Institute of Technology Ladkrabang, Thailand.
s5060204@kmitl.ac.th, kwwithaw@kmitl.ac.th,
kpchucha@kmitl.ac.th, ksamanas@kmitl.ac.th

ABSTRACT

Image registrations have been a subject of extensive study over the last decade. They appear in numerous applications including Computer Vision, Pattern Recognition, Medical Image Analysis and Remotely Sensed Image Processing. We introduce a non-iterative geometric-based method to register an image using a novel set of geometric landmarks residing on an extracted 2D contours from the image. These landmarks are intrinsic and are computed from the differential geometry of the curve. We exploit the invariant properties of maximum-curvature points that are local and preserved under the affine and some perspective transformation. Geometric invariant exploits coplanar five-point invariant constructed from 4 consecutive landmarks and a centroid. This invariant is preserved not only in affine map but weak perspective map as well. To reduce the sensitivity of the landmarks to noise, we use a B-Spline surface representation that smoothes out the curve prior to the computation of the landmarks. The alignment is achieved by establishing correspondences between the landmarks after a conformal sorting based on derived absolute invariant. The experiments have shown that the purposed methods are robust and promising even in the presence of noise.

KEYWORDS: Image Registration, Perspective Transformation, Invariant, B-spline, Contour alignment

1. INTRODUCTION

Image registration is a vital step in many tasks, such as data fusion, change detection, pose recovery, etc., and have been investigated in various contexts. It is also crucial in molecular biology for the binding of the ligands and receptors in synthetic drug design. Both therapy planning and evaluation require global surface registration methods for integrating medical images obtained from different modalities. This is an important step in performing comparative studies on the same patient over different stages of analysis, as well as on different patients. For example, in clinical diagnostic of cancer radiation treatment planning

requires the merging sophisticated imaging modalities such as computerized tomography (CT) and magnetic resonance imaging (MRI) which provides complementary information for localization and characterization of the tumor and normal tissue. In epilepsy surgery planning, EEG (Electroencephalograph), MRI and SPECT (Single Photon Emission Computerized Tomography) are combined.

Image registration methods can be categorized into intensity-based and feature-based method. The intensity-based registration created a cost function from voxel intensity space directly and iteratively optimizing this function among different transformation parameters. To avoid falling into local minima, most of this method requires initial alignment prior to performing the registration. One of the pioneered works in intensity-based method was done by Wood et.al. [Woo92a], [Woo93a]. Woods and his colleagues used the standard deviation of the pixel values that corresponds to each MRI pixel values as the cost function to perform both linear (rigid body, affine) or nonlinear (polynomial), allowing inter- and intra-modality alignment. Viola and Wells [Vio95a] studied the MRI alignment by maximizing mutual information. This method has

Permission to make digital or hard copies of all or part of this work for personal or classroom use is granted without fee provided that copies are not made or distributed for profit or commercial advantage and that copies bear this notice and the full citation on the first page. To copy otherwise, or republish, to post on servers or to redistribute to lists, requires prior specific permission and/or a fee.

Journal of WSCG, Vol.12, No.1-3, ISSN 1213-6972
WSCG'2004, February 2-6, 2003, Plzen, Czech Republic.
Copyright UNION Agency – Science Press

been found to be very effective in 3D-to-3D multi-modal image registration between modalities such as MRI and PET, or MR and CT [Mae97a], [Stu96a],[Stu97a]. But the performance degrades in 2D-to-3D alignment. Others works on intensity-based approach can be found, according to the applied cost function, in normalized cross correlation [Mem94a], entropy of difference image [Buz97a], gradient correlation [Bro96a], and pattern intensity [Wee97a].

The feature-based method generally involves extracting corresponding (or equivalent in some cases) features from the images to be registered and estimate the transformation parameters that relates to those corresponding features. Feature-based approach can be classified into surface symmetry detection, high order polynomial representation, invariance-based approaches, distance map technique, energy-base method, landmark-mapping techniques and boundary/line mapping methods. Surface symmetry based registration exploits the various symmetries in the surface under study [Sun97a]. Their performance degrades, in general, in partial matching situations as the degree of symmetries are weakened. High order polynomial-based matching [Sve76a] models the surface by implicit polynomials. To capture the complex surface, such as brain structure, high order polynomials are needed which presents a stability problem. This is particularly the case in the presence of noise, local deformations and partial matching. Invariance-based methods rely on extracting cues and shape features (2D or 3D) that are preserved under a class of transformations. The most widely used is geometric invariance analysis [Mun92a]. Geometric invariance could be a complicated process [Zis92a] for general surfaces.

Distance map technique uses a metric that measures the distance between different sets of points. In this method, an iterative procedure looks for the closest point in a set of data to a sample point, computes the transformation that registers the points and applies the transformation to the data primitives. In general, distance map approaches are very suitable to deal with incomplete data, but the process becomes very cumbersome in the presence of transformations that are more general than rigid (similarity, affine and weak perspective). Pelizzari and his colleagues [Pel89a] developed an automated algorithm for matching 3D surfaces derived from different modalities. The method recovered geometric transformation by minimizing a residual error that is a mean squared distance between the points from MR and the contours from CT. To guarantee convergence to a global minimum, this method requires a rough initial registration. Grimson *et al* [Gri96a] developed a technique, which does not require operator intervention to set an initial starting position. To avoid a local minimum, they randomly

perturb near final solutions. For other works on this method not discussed here, see [Bes85a], [Bes92a], [Lav92a], [Cal96a], [Koz97a] and [Mau98a].

Energy-based registration is the class of registration that is based on theory of mechanics. According to the theory of mechanics the deformed object has energy that is a function of strain, stress and displacements. If one wants to bring the object in alignment, one has to bring the object in equilibrium. Bajcsy and Broit [Bro81a] introduced the theory of deformation of elastic solid in the area of brain mapping. They seek to find the displacements that give the deformed (equilibrium) state of the object by using equilibrium equation of elastic solid as a constraint. Terzopolulos *et al* [Ter87a] purposed energy constraints on deformable models for recovering shape and non-rigid motion. The active contours (called snakes) have been used for solving computer vision problem based on energy minimization framework, which were later adopted in the area of image registration by several authors [Por94a], [Tho96a]. More works on energy-based method can be found in [Met91a], [Sta96a], [Coh96a], [Thi99a], and [Gab98a]. See also [Fel96a] where a combination of energy-based and distance map method was proposed for the alignment in the presence of a nonrigid transformation.

Landmark-mapping alignment involves the determination of the coordinates of the corresponding points in different images and the estimation of the geometrical transformation using these corresponding points. These landmarks could be anatomical structures, e.g., rhinal fissure, the fundus beds, etc., or geometric points. The geometric points are virtual fiducials, and are based on the differential geometry of the surface. Typical geometric features include line intersections [Sto82a], local curvature maxima, [Van98a] and [Kan81a], centroid of closed-boundary region [Gos86a], extremal points [Thi96a], knot points [Coh98a], and zero-curvature points [Mun92b]. A combination of fiducial marks and anatomical surface features was proposed, [Col94a] and [22], for alignment in the presence of a rigid transformation. In [Jac96a] a set of landmarks obtained from 2D images is arranged in a 3D geometric hash table to provide analytical surface description. Generalized Hough transforms (pose clustering) were used in [Sto87a] for calculating the object pose from a set of landmarks associated with a model. Pose clustering is generally a computationally intensive process. Moreover, in brain image registration, the insertion of artificial fiducially points is either difficult or may be undesirable.

Boundary and line mapping methods uses active contours to establish a homothetic map between sets

of boundaries before a 2D elastic transformation is found [Dav96a]. Ridge lines extracted from 3D images, are used to build a crest lines' atlas and are used for brain surface registration techniques [Sub94a], [Mai96a]. Ridge lines are based on maximal curvature, which is preserved only under similarity transformation. Govindu and Shekar [46] exploited geometric information on the image contours to estimate the relevant transformation between images by maximizing the similarity of the distribution of local geometric properties such as curvature. This method does not require explicit feature correspondence.

In this paper we will introduce a novel method which is a combination of invariant and geometric landmark based registration techniques. We study local geometric intrinsic features from which we derive a set of fiducial points which are the maximum-curvature points. These landmarks points are preserved under affine and some perspective transformation. Compared with zero-curvature points used by walid *et.al.* [Wal98a], the maximum-curvature points are more robust to noise. Moreover, threshold of curvature can be set such that only the maximum-curvature point of which its curvature exceedings the threshold are selected. As a result, maximum-curvature points caused by local disturbance are excluded. To establish the correspondence between two sets of fiducially points, local geometric projective (affine and weak perspective) invariants are constructed, which are extracted from the five point coplanar [Eam91a] spanned by the landmark point. Unlike previous works on landmark extraction using differential geometry (e.g., Subsol *et al.*'s work on crest (ridge) lines and crest points [Sub94a]), the curve landmarks that are introduced in this paper are intrinsic, local, and preserved under affine warping. Our purposed approach does not depend on the expert extraction of biological landmarks. These are automatically extracted from the curve representation. Our method does NOT need an iterative approach to establish the warping transformation. It directly computes (closed-form solution) from the corresponding landmarks.

This paper is organized as follows. A brief overview of B-Spline Curve modeling is given in Section I. Section II introduces the local geometric surface features used as landmarks on the curve. The registration process is thoroughly discussed in section IV. Experimental results are shown in section V. Discussion and conclusions are presented in section VI.

2. B-SPLINE MODELING

A p^{th} degree non-rational B-spline curve is defined as follows

$$r(t) = \sum_{i=0}^n N_{i,p}(t)P_i \quad a \leq t \leq b \quad (2.1)$$

Where the $\{P_i\}$ are the control points and The $N_{i,p}(t)$ are the p^{th} -degree B-spline functions defined by equation (2.1) defined on the non-periodic (and non-uniform) knot vector.

$$U = \{\underbrace{a, \dots, a}_{p+1}, u_{p+1}, \dots, u_{m-p-1}, \underbrace{b, \dots, b}_{p+1}\} \quad (2.2)$$

Unless stated otherwise, $a=0$ and $b=1$. The number of knots is related to the number of control points and the degree by the formula $m = n + p + 1$. The polygon formed by $\{P_i\}$ is called the control polygon.

B. Why B-splines

The B-spline curve has superior properties that make them suitable for shape representation and analysis. Some of the important properties are:

(i) Smoothness and continuity: Due the differentiability properties of the basis B-spline function, the B-spline curve is at least continuously differentiable of up to $p - 1$ times. For the cubic B-spline curve, for example, the 2^{nd} derivative B-spline curve exists.

(ii) Boundedness: The B-spline curve is confined in the convex hull of its control polygons. In fact, for t in the knot span $[t_i, t_{i+1})$, the $r(t)$ is bounded by the convex hull of the control points p_{i-p}, \dots, p_i .

(iii) Local shape controllability: Due to the local support of the basis B-spline function, moving p_i affects $r(t)$ only in the interval $[t_i, t_{i+p+1})$ and hence the change of shape produced by varying one of p_i is locally confined.

(iv) Affine (projective) invariance: a B-spline subjected to an affine (projective) transformation is still a B-spline whose control points are obtained by subjecting the original B-spline control points to that affine (projective) transformation.

3. INTRINSIC GEOMETRIC FEATURES OF CURVE

Our geometric landmarks are computed from the differential geometry of the curve. The zero curvature points or the inflection points are relative invariant and have been used as the candidates for curve matching [Ric91, Wal98a]. The zero-curvature point, however, is relatively sensitive to noise [Wal98a]. In this paper, we use maximum curvature point as our fiducial point.

For a curve parameterized by t (chord length not arc length), the curvature is defined as

$$k(t) = -\frac{|r^{(1)}(t) \times r^{(2)}(t)|}{|r^{(1)}(t)|^3} \quad (3.1)$$

The zero-curvature point is the point where the curvature is zero; i.e. the points at which

$$\begin{aligned} k(t) &= -\frac{|r^{(1)}(t) \times r^{(2)}(t)|}{|r^{(1)}(t)|^3} = 0 \\ &= |r^{(1)}(t) \times r^{(2)}(t)| = 0 \end{aligned} \quad (3.2)$$

For an affine transformed curve $r'(t)$ where $r'(t) = [T] \cdot r(t)$ and where T is an affine transformation matrix, the curvature of an affine-affine transformed curve is hence

$$k(t) = -\frac{|[T]r^{(1)}(t) \times [T]r^{(2)}(t)|}{|[T]r^{(1)}(t)|^3} \quad (3.3)$$

The zero-curvature point of the affine transformed curve is hence

$$\begin{aligned} k(t) &= -\frac{|[T]r^{(1)}(t) \times [T]r^{(2)}(t)|}{|[T]r^{(1)}(t)|^3} = 0 \\ &= |[T]r^{(1)}(t) \times [T]r^{(2)}(t)| = 0 \\ &= |r^{(1)}(t) \times r^{(2)}(t)| = 0 \end{aligned} \quad (3.4)$$

This is the same as equation as (3.2) before undergoing the transformation. Thus the zero-curvature points are preserved under the affine group.

The maximum-curvature point is the point where the curvature is at the peak. By taking derivation of the curvature, the maximum-curvature point will be the point where the derivation of the curvature is zero, i.e. the point at which

$$\begin{aligned} |r^{(3)}(t)|^3 |r^{(1)}(t) \times r^{(2)}(t)|^{(1)} \\ - |r^{(1)}(t) \times r^{(2)}(t)| \left(|r^{(3)}(t)|^3 \right)^{(1)} = 0 \end{aligned} \quad (3.5)$$

Similarly, the maximum-curvature point of an affine-transformed curve is the point at which

$$\begin{aligned} |[T]r^{(3)}(t)|^3 |[T]r^{(1)}(t) \times [T]r^{(2)}(t)|^{(1)} \\ - |[T]r^{(1)}(t) \times [T]r^{(2)}(t)| \left(|[T]r^{(3)}(t)|^3 \right)^{(1)} = 0 \\ |r^{(3)}(t)|^3 |r^{(1)}(t) \times r^{(2)}(t)|^{(1)} \\ - |r^{(1)}(t) \times r^{(2)}(t)| \left(|r^{(3)}(t)|^3 \right)^{(1)} = 0 \end{aligned} \quad (3.6)$$

This is the same as equation as (3.5) before undergoing the transformation. Thus the maximum-curvature points are preserved under the affine group.

4. CONSTRUCTING ABSOLUTE INVARIANT USING ZERO-CURVATURE AND MAXIMUM-CURVATURE POINTS

Geometric invariants are shape descriptors that remain unchanged under geometric transformations such as perspective and affine transformation that will be used mainly as object recognition and/or image registration. A new approach of obtaining the invariants has been developed and used in the curve matching and recognition. A maximum-curvature point which is the local and invariant intrinsic property of the curve can be uniquely identified both before and after transformation. The identified maximum-curvature points then are used to compute the geometric invariants which serve as the curve signature for the curve matching and recognition. The well-known perspective invariant is five-point coplanar.

Any five nonlinear points in the plane, namely P_1, \dots, P_5 can also form perspective invariant- the so-called five-point coplanar [Eam91a] with their image, P'_1, \dots, P'_5 ,

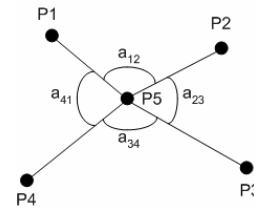


Figure 1. Five points

$$\frac{|m'_{431}| |m'_{521}|}{|m'_{421}| |m'_{531}|} = \frac{|m_{431}| |m_{521}|}{|m_{421}| |m_{531}|} \quad (4.1)$$

where $m_{ijk} = (P_i \ P_j \ P_k)$ with $P_i = (x_i \ y_i \ 1)^T$, $m'_{ijk} = (P'_i \ P'_j \ P'_k)$ with $P'_i = (x'_i \ y'_i \ 1)^T$ and $|m|$ is the determinant of m . Consider any one of the matrices in (4.1)

Since the invariant relationship in equation (4.1) holds under a perspective transformation, a set of perspective invariant can be constructed by considering 4 consecutive maximum-curvature points and a centroid which is also preserved under an affine and perspective transformation. For a curve with n maximum-curvature points, there are n set of geometric invariants denoted as $I_{fp}(k)$ for $k = 1, 2, \dots, n$

5. ESTABLISHING CORRESPONDENCE AND ALIGNMENT

The registration process is carried out in the presence of an affine transformation and a possible perspective transformation. We first compute the curve intrinsic feature points (maximum-curvature points). The relative invariant and absolute invariants explained in section 4 is computed. The correspondence between the feature points on the original and the transformed curve is established. From this correspondence, the transformation parameters are computed and the transformed curve is aligned against an original.

In the absence of noise, occlusion, each of $I_a(j)$ of (4.1) will have a counterpart $I(i)$ with $I_a(j) = I(i)$, with that counterpart easily determined through a circular shift involving n comparison where n is the number of invariant. In the presence of non-linear transformation, we allow smaller error percentage between counterpart invariant. Having a smaller threshold will force this run length matching technique to allow for only small difference between the volume patch before declares them as matching. This may reduce the length of the matched sequence element, Thus the lower the error percentage, the more strict the matching. Experimentally, an error percentage of 5% was applied. We adopted a run length method to decide on the correspondence between the two ordered set of maximum curvature point. For every starting point on the transformed, this run length method computes a sequence of consecutive invariant that satisfies $|I(i) - I_a(j)| < 0.05|I(i)|$ and declare a match based on the longest string. Once this correspondence is found, these matched landmarks are used to estimate the transformation matrix.

6. EXPERIMENT

Two applications are illustrated in this paper to show the capabilities of the image registration exploiting five-point coplanar perspective invariant and maximum-curvature point. The first experiment is the alignment of brain contours subject to the rigorous

transformation and noise whereas the second experiment is the classification of various fish shapes.

6.1 Brain Alignment

The contour of brain shown in Figure 1 is used to demonstrate the application of alignment. It contains 960 points of data extracted from the cross section of actual brain. Three conditions are set up to severely alter the shape of contour. These conditions include the affine transformation, the perspective transformation, and the noise disturbance. The affine transformation generally consists of scaling, transformation, rotation, and shearing. The parameters of affine transformation used in the experiment are described by the following equation

$$\begin{bmatrix} x'_1 & y'_1 & 1 \\ \vdots & \vdots & \vdots \\ x'_N & y'_N & 1 \end{bmatrix} = \begin{bmatrix} x_1 & y_1 & 1 \\ \vdots & \vdots & \vdots \\ x_N & y_N & 1 \end{bmatrix} \begin{bmatrix} sx & 0 & 0 \\ 0 & sy & 0 \\ 0 & 0 & 1 \end{bmatrix} \times$$

$$\begin{bmatrix} 1 & shx & 0 \\ shy & 1 & 0 \\ 0 & 0 & 1 \end{bmatrix} \begin{bmatrix} \cos \theta & \sin \theta & 0 \\ -\sin \theta & \cos \theta & 0 \\ 0 & 0 & 1 \end{bmatrix} \quad (6.1)$$

where (x', y') is the transformed coordinates, (x, y) is the original coordinates, N is number of points, sx , sy , shx , shy , and θ are 1.5, 1.5, 0.5, 0.3, and π respectively.

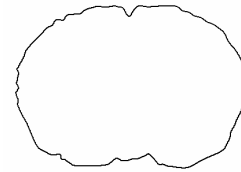


Figure 2. Original brain contour

The perspective transformation is the generalized version of the affine transformation; it includes all the affine parameter and the perspective parameter. The experimental parameters for perspective transformation are written in Equation 6.2.

$$\begin{bmatrix} x'_1 & y'_1 & 1 \\ \vdots & \vdots & \vdots \\ x'_N & y'_N & 1 \end{bmatrix} = \begin{bmatrix} x_1 & y_1 & z_1 & 1 \\ \vdots & \vdots & \vdots & \vdots \\ x_N & y_N & z_N & 1 \end{bmatrix} \times$$

$$\begin{bmatrix} 1 & 0 & 0 & 0 \\ 0 & \cos \theta & \sin \theta & 0 \\ 0 & -\sin \theta & \cos \theta & 0 \\ 0 & 0 & 0 & 1 \end{bmatrix} \begin{bmatrix} 1 & 0 & 0 \\ 0 & 1 & 0 \\ 0 & 0 & 1/d \\ 0 & 0 & 0 \end{bmatrix} \quad (6.2)$$

Where (x', y') is the transformed coordinates, (x, y, z) is the original coordinates, θ and d are 20° and 500 respectively.

For the noise disturbance, the SNR of the Gaussian-distributed noise is equal to 30 dB. The contour with the presence of noise is shown in Figure 2.

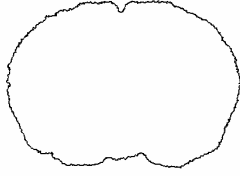


Figure 3. The brain contour distorted by noise with SNR of 30 dB.

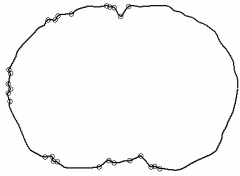


Figure 4. B-spline fitted brain contour with the positions of maximum curvatures marked by "o".

Three altered contours and one original contour are fitted by the third order B-spline curve with 30 control points. After that, the set of maximum-curvature points is extracted. In Figure 3, the locations of maximum curvatures are marked by "o" signs. These points of curvatures are implied as the landmarks having the relative invariant feature. With the property of five-point coplanar scheme, the absolute invariant feature can be found explicitly. This feature helps locate the corresponding points on the contour.

Condition	Error of Registration
Affine Transformation	0.0000
Perspective Transformation	2.0828
Noise Disturbance	4.3917

Table 1. Error of the registered images in three conditions.

Table 1 shows the errors of the registered images in three different conditions. The errors are measured from the difference of distance between original points and registered points using Equation 6.3.

$$Error = \frac{\sum_{i=1}^N (|P_{oi} - P_{ri}|)}{N} \quad (6.3)$$

6.2 Fish Classification

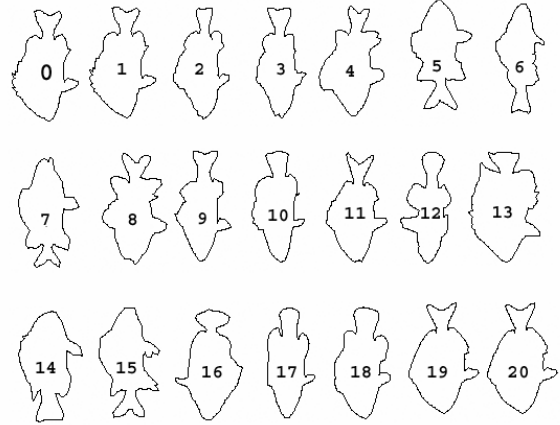


Figure 5. Twenty-one shapes of fish used for classification.

Twenty-one contours of fish which have the various patterns are shown in Figure 4. Each contour has approximately 400 points of coordinates. Again, the third order B-spline with control points of 30 is employed to fit the contours of fish. To find the fish which matches with the 0th fish, the sequences of 5-point coplanar of all fish are determined from the maximum curvature and a centroid. The sequences of other fish are compared to the sequence of the 0th fish and searched for the closest segments. The errors of closest segments which have the length of 4 and 5 are shown in Table 2. Note that the 1st fish has the minimum error among the others.

Fish Number	Segment Length	
	4	5
1	2.5284	2.9543
2	4.7719	4.5184
3	5.2004	7.2602
4	5.9368	7.7671
5	6.5661	11.3461
6	3.0231	8.4538
7	5.5171	10.2837
8	5.0336	4.6320
9	6.7639	8.4016
10	4.6308	6.2769
11	5.8852	10.4255
12	4.3167	5.6883
13	3.7194	6.5285

14	3.4117	7.5764
15	7.2079	6.6701
16	5.6181	6.8631
17	3.1261	4.3881
18	3.7787	6.8962
19	6.0924	7.1570
20	5.3986	8.5795

Table 2. Errors of the closest segment in the 5- point coplanar sequences.

7. DISCUSSION AND CONCLUSION

This paper we explore the invariant property of the maximum-curvature points. The fact that the maximum-curvature points are local and preserved under an affine transformation makes them feasible to use for matching and classification of curve. By exploiting the absolute affine and perspective invariant using the feature points, the correspondence between the feature points on the original and the transformed curve is established, the transformation parameters are computed and the transformed curve is aligned against an original. We also enjoy the benefit of curve representation by B-splines as B-splines processes very attractive properties. B-splines are smooth, continuous, and consists of continuously connected pieces each described by a low order polynomial in the parameters, yet it is presented as a single unit. B-splines have local controllability which implies that local changes in shape are confined to the B-spline parameters local to that change. More importantly, B-splines are shape invariance under affine transformation.

8. REFERENCE

- [Bar91a] E.B. Barrett and P. Payton, "General Methods for Determining Projective Invariants in Imagery", *CVGIP: Image Understanding*, Vol. 53, No. 1, pp. 46-65, Jan. 1991.
- [Bes85a] Besl, P. J. and Jain, R. C., "Three-dimensional Object Recognition," *ACM Comput. Surv.*, 17, 1, pp. 75-154, 1985.
- [Bes92a] Besl, P. J. and McKay, N. D., "A Method for Registration of 3D Shapes," *IEEE Trans. Patt. Anal. Machine Intell.*, 14, 2, pp. 239-256, 1992.
- [Boo78a] De Boor, C., *A Practical Guide to Splines*, New York: Springer-Verlag, 1978
- [Bro81a] Broit, C., "Optimal Registration of Deformed Images," Doctoral Dissertation, Univ Pennsylvania, 1981.
- [Bro96a] Brown, L. M. G., and Boulton, T. E., "Registration Planar File Radiographs with Computed Tomography," in *Proc. MMBIA*, 1996, pp. 401-412.
- [Buz97a] Buzug, T. M., Weese, J., Fassnacht, C., and Lorenz, C., "Image Registration Convex Weight Functions for Histogram-based Similarity Measures," in *Proc. CVRMed/MRCAS*, Trocraz, J., Greimson, E., and Mosges, R., Eds, Berlin, German: Springer-Verlag, 1997, pp. 203-212.
- [Cal96a] Calvin, R. M. Jr., Aboutanos, G. B., Dawant, B. M., Maciunas, R. J. and Fitzpatrick, J. M., "Registration of 3D Images using Weighted Geometric Features," *IEEE Trans. on Med. Imaging*, 15, 6, pp. 836-849, 1996.
- [Car76a] Do Carmo, M. P., *Differential Geometry of Curves and Surfaces*, Prentice Hall, Englewood Cliffs, NJ 1976.
- [Coh96a] Cohen, L.D., "Deformable Surfaces and Parametric Models to Fit and Track 3D Data," *In IEEE International Conference on Systems, Man and Cybernetics*, 4, pp. 2451-2456, 1996.
- [Coh98a] Cohen, F. S., Yang, Z., Huang, Z. and Nissanov, J., "Computer Matching of Histological Rat Brain Sections," *IEEE Trans. on Biomedical Engineering* 45, 5, pp. 642-649, 1998.
- [Coh00a] Cohen, F. S., Ibrahim, W., Pintavirooj, C., "Ordering and Parameterizing Scattered 3D Data for B-Spline Surface Approximation," *IEEE Transactions on Pattern Analysis and Machine Intelligence*, vol. 22, no. 6, pp. 642-648, 2000.
- [Col94a] Collignon, A., Vandermeulen, D., Suetens, P. and Marchal, G., "Registration of 3D Multi-Modality Medical Images using Surfaces and Point Landmarks," *Pattern Recognition Letters*, vol. 15, pp. 461-467, May 1994.
- [Dav96a] Davatzikos, C., Prince, J. L., Bryan, R. N., "Image Registration based on Boundary Mapping," *IEEE Trans. on Med. Imaging*, 15, 1, pp.112-115, 1996.
- [Eam91a] Eamon B. Barrett, Paul M. Payton, "General Methods for Determining Projective Invariants in Imagery," *Image Understanding*, vol. 53, pp. 46-65, 1991.
- [Fel96a] Feldmar, J. and Ayache, N., "Rigid, Affine and Local Affine Registration of Free Form Surfaces," *Int. J. of Patt. Recog.*, 18, 2, pp. 99-119, 1996.
- [Gab98a] Gabrani, M., "Multidimensional Spline Interpolation Theory and Surface-based Alignment of Brains," Doctoral Dissertation, Drexel Univ, 1998.
- [Gos86a] Goshtasby, A., "Piecewise Linear Mapping Functions for Image Registration," *Patt. recog.*, 19, 6, pp. 459-466, 1986
- [Gov99a] Govindu, V. and Shekhar, C., "Alignment using Distributions of Local Geometric Properties," *IEEE Trans. Patt. Anal. Machine Intell.*, vol. 21, no. 3, pp.1031-1043, 1999.
- [Gri96a] Grimson, W. E. L., Ettinger, G. J., White, S. J., Lozano-Perez, T., Wells, W. M. and Kikinis, R., "An Automatic Registration Method for Frameless, Stereotaxy, Image Guided Surgery and Enhanced Reality Visualization," *IEEE Trans. on Med. Imaging*, 15, 2, pp. 129-140, 1996
- [Jac96a] Jacobs, D. W., "The Space Requirements of Indexing under Perspective Projections," *IEEE Trans. Patt. Anal. Machine Intell.*, 18, 3, pp.330-333, 1996.
- [Kan81a] Kanal, L. N., Lambird, B. A., Lavine, D. and Stockman, G. C., "Digital Registration of Images from Similar and Dissimilar Sensors," *In Proceedings of the International Conference on Cybernetics and Society*, pp. 347-351, 1981.

- [Koz97a] Kozinska, D., Tretiak, O. J., Nissanov, J. and Ozturk, C., "Multidimensional Alignment using the Euclidean Distance Transform," *Comput. Vision. Graph. Image Process.*, 59, 6, pp. 373-387, 1997.
- [Lav92a] Lavallee, S. and Szeliski, R., "Recovering the Position and Orientation of Free-form Objects from Image Contours using 3D Distance Maps," *IEEE Trans. Patt. Anal. Machine Intell.*, 17, 4, pp. 378-390, 1992.
- [Mae97a] Maes, F., Collingnon, A., Vandermeulen, D., Marchal, G., and Seutens, P., "Multimodality Image Registration by Maximization of Mutual Information", *IEEE Trans Med. Imag.*, vol. 16, pp.187-190, 1997
- [Mai96a] Maintz, J. B., van den Elsen, P. A., and Viergever, M. A., "Evaluation of Ridge Seeking Operator for Multi-modality Medical Image Matching," *IEEE Trans. Patt. Anal. Machine Intell.*, vol. 18, no. 3, pp.354-365, 1996.
- [Mau98a] Maurer C. R., Jr., Maciunas R. J., Fitzpatrick, J. M., "Registration of Head CT Images to Physical Space using Weighted Combination of Points and Surfaces," *IEEE Trans. on Med. Imaging*, 17, 5, pp. 753-761, 1998.
- [Mem94a] Memieux, L., Jagoe, R., Fish, D. R., Kitchen, N. D., and Thomas, D. G. T., "A patient-to-computed-tomography Image Registration Method based on Digitally Reconstructed Radiographs," *Med. Phys.*, vol. 21, no.11, pp 1749-1769, 1994
- [Met91a] Metaxas, D. and Terzopoulos, D., "Constrained Deformable Superquadrics and Nonrigid Motion Tracking," *In IEEE proceedings of computer vision and pattern recognition*, pp. 337-343. *IEEE computer Society Conference*. Lahaina, Maui, Hawaii., 1991.
- [Mun92a] Mundy, J. and Zisserman, A., Editors, *Geometric Invariance in Machine Vision*, MIT Press, 1992.
- [Mun92b] Mundy J. L. and Zisserman A., *Geometric Invariance in Computer Vision*, MIT press, 1992.
- [Pel89a] Pelizzari, C. A., Chen, D. T. Y., Spelbring, D. R., Weichselbaum, R. R., and Chen, C. T., "Accurate Three-dimensional Registration of CT, PET, and/or MR Images of the Brain," *J. Comput. Assisted Tomogr.*, 13, 1, pp. 20-26, 1989.
- [Por94a] Porrill, J. and Ivins, J., "A Semiautomatic tool for 3-D Medical Image Analysis using Active Contour Models," *Med. Inform.*, vol. 19, no.1, pp.81-90, 1994.
- [Sta96a] Staib, L. H., Duncan, J. S., "Model-based Deformable Surface Finding for Medical Images," *IEEE Trans. on Med. Imaging*, 15, 5, pp. 720-731, 1996.
- [Sto82a] Stockman, G.C., Kopstein, S., and Bennett, S., "Matching Images to Models for Registration and Object Detection via Clustering," *IEEE Trans. Patt. Anal. Machine Intell.*, 4, pp.229-241, 1982
- [Sto87a] Stockman, G. C., "Object Recognition and Localization via Pose Clustering," *Comput. Vision. Graph. Image Process.*, 40, pp. 361-387, 1987.
- [Stu96a] Studhome, C., Hill, D. L. G., and Hawkes, D. J., "Automated 3D Registration of MR and CT Images of the Head," *Med. Image. Anal.*, vol.1 no.2, pp. 163-175, 1996
- [Stu97a] Studhome, C., Hill, D. L. G., and Hawkes, D. J., "Automated 3D Registration of MR and PET Images by Multi-resolution Optimization of Voxel Similarity Measures," *Med. Phys.*, vol.24, pp. 25-35, 1997
- [Sub94a] Subsol, G., Thirion, J. P. and Ayache, N., "Non Rigid Registration for Building 3D Anatomical Atlases" *In Proceedings of the 12th IAPR International Conference on Pattern Recognition. Conference A: Computer Vision & Image Processing*, vol. 1, pp. 576-578, 1994.
- [Sun97a] Sun, C. and Sherrah, J., "3D Symmetry Detection using the Extended Gaussian Image," *IEEE Trans. Patt. Anal. Machine Intell.*, PAMI, vol. 19, no.2, pp. 164-168, February 1997.
- [Sve76a] Svedlow, M., Mcgillum, C. D., and Anuta, P. E., "Experimental Examination of the Similarity Measures and the Prepropossing Methods used for Image Registration", *In the Symposium on Machine Processing of Remotely Sensed Data*, Westville, Ind., pp. 4A-9, June, 1976.
- [Ter87a] Terzopoulos, D., Witkin, A. and Kkass, M., "Energy Constraints on Deformation models: Recovering Shape and Non-rigid Motion," in *Proc.*, AAAI 87, vol2, pp.775-760, July 1987.
- [Thi96a] Thirion, J. P., "New Feature Points based on Geometric Invariants for 3D Image Registration," *Int. J. of Patt. Recog.*, 18, 2, pp. 121-137, 1996.
- [Thi99a] Thirion, J. P. and Calmon, G., "Deformation Analysis to Detect and Qualifying Active Lesions in three-dimensional medical images sequences," *IEEE Trans. on Med. Imaging*, 18, 5, pp. 429-441, 1999.
- [Tho96a] Thompson, P. and Toga, A. W., "A Surface-based Technique for Warping Three-dimensional Images of the Brain," *IEEE Trans. on Medical Imaging*, vol. 15, no. 4, 1996.
- [Van98a] Van Essen, D. C. and Drury, H.A., Joshi, S. and Miller, M., "Functional and Structural Mapping of the Human Cerebral Cortex: Solution are in the surface," *In Proceedings of the National Academy of Science.*, 95, pp.788-795, 1998.
- [Vio95a] Viola, P. and W. M. Wells, W. M., "Alignment by Mmaximization of Mutual Information," in *Proc. 5th Int. Conf. On Computer Vision (ICCV'95)*, pp. 16-23, 1995.
- [Wal98a] Walid S. Ibrahim Ali, Fernand S. Cohen, "Registering Coronal Histological 2-D Sections of a Rat Brain with Coronal Sections of a 3-D Brain Atlas Using Geometric Curve Invariants and B-Spline Representation," *IEEE Transactions on Medical Imaging*, vol. 17, no. 6, December 1998.
- [Wee97a] Weese, J., Buzug, T. M., Lorenz, C., and Fassnacht, C., "An Approach to 2D/3D Registration of a Vertebra in 2D X-ray Fluoroscopies with 3D CT Images," in *Proc CVRMed/MRCAS*, 1997, pp. 119-128.
- [Woo92a] Woods, R. P., Cherry, S. R., Mazziotta, J. C., "Rapid Automated Algorithm for Alignment and Reslicing PET Images," *J. Comput. Assist Tomogr.*, vol. 16, pp. 620-633, 1992.
- [Woo93a] Woods, R. P., Mazziotta, J. C., and Cherry, S. R., "MRI-PET Registration with Automated Algorithm," *J. Comput. Assist Tomogr.*, vol. 17, no 4, pp. 536-546, 1993.
- [Zis92a] Zisserman, A., Forsyth, D. A., Mundy, J. L., Rothwell, C. A., "Recognizing General Curved Objects Efficiently," in *Geometric Invariance in Machine Vision*, pp.228-252, Mundy, J. and Zisserman, A., Editors, MIT Press, 1992.